Molecular Crystals and Liquid Crystals Science and Technology. Section A. Molecular Crystals and Liquid Crystals

Publication details, including instructions for authors and subscription information:
http://www.tandfonline.com/loi/gmcl19

Solid State Amorphization of Organic Crystals and Thermodynamic Properties of the Amorphized Solids

Osamu Yamamuro [a] , Itaru Tsukushi [a] & Takasuke Matsuo [a]

[a] Department of Chemistry and Microcalorimetry Research Center, Faculty of Science, Osaka University, Toyonaka, Osaka, 560, Japan

Version of record first published: 04 Oct 2006.

To cite this article: Osamu Yamamuro , Itaru Tsukushi & Takasuke Matsuo (1996): Solid State Amorphization of Organic Crystals and Thermodynamic Properties of the Amorphized Solids, Molecular Crystals and Liquid Crystals Science and Technology. Section A. Molecular Crystals and Liquid Crystals, 277:1, 205-214

To link to this article: http://dx.doi.org/10.1080/10587259608046023

Mol. Cryst. Liq. Cryst., 1996, Vol. 277, pp. 205–214
Reprints available directly from the publisher
Photocopying permitted by license only

SOLID STATE AMORPHIZATION OF ORGANIC CRYSTALS AND THERMODYNAMIC PROPERTIES OF THE AMORPHIZED SOLIDS*

OSAMU YAMAMURO, ITARU TSUKUSHI AND TAKASUKE MATSUO
Department of Chemistry and Microcalorimetry Research Center, Faculty of Science, Osaka University, Toyonaka, Osaka 560, Japan

Abstract The organic crystals of tri-*O*-methyl-β-cyclodextrin (TMCD) and its three clathrate compounds containing benzoic acid (BA), *p*-nitrobenzoic acid (NBA) and *p*-hydroxybenzoic acid (HBA), sucrose (SUC), salicin (SAL), phenolphthalein (PP), 1,3,5-tri-α-naphthylbenzene (TNB) were amorphized by grinding with a vibrating mill for 2-16 h at room temperature. The amorphization was checked by differential scanning calorimetry (DSC) and X-ray powder diffraction. The heat capacities of crystals, liquid quenched glasses (LQG), and ground amorphous solids (GAS) of TMCD and TNB were measured with an adiabatic calorimeter in the temperature range between 12 and 375 K. For both compounds, the enthalpy relaxation of GAS followed quite unusual temperature evolution and the released configurational enthalpy was much larger than that of LQG, indicating that GAS is more disordered and strained than LQG. The grinding-time and grinding-temperature dependences on the enthalpy relaxation were also investigated for TMCD. It was found that the latter effect is more important than the former.

INTRODUCTION

Amorphous solids are usually prepared by quenching their liquids or depositing their vapors on a cold substrate. Recently solid state amorphization has been recognized as the third group of amorphization technique.[1,2] This is the process from the opposite side to the conventional procedure, *i.e.*, supplying energy to disturb an equilibrium crystal and freeze it in an energized metastable amorphous state. Most of the studies done so far concern binary alloys of transition metals (Ni, Zr, *etc.*)[3] and inorganic compounds (SiO_2, *etc.*).[4] The solid state amorphization of tri-*O*-methyl-β-cyclodextrin has been studied from the pharmaceutical interest in relation to the solid-state inclusion of drugs.[5] Mechanical grinding in a ball mill and irradiation of high energy electron or neutron beam are commonly-used techniques for solid state amorphization.

We have applied the mechanical grinding to several organic molecular crystals. The molecular crystals are formed by weak intermolecular forces such as van der Waals interactions. Consequently, the difference between the Gibbs energies of crystalline and liquid phases is small. By expending a relatively small amount of mechanical energy, one may increase the free energy of the crystal to that of the supercooled liquid. If we do this

at a temperature below the glass transition temperature of the substance, the resulting amorphous state may be glassy rather than the supercooled liquid.

The substances investigated before are as follows: tri-*O*-methyl-β-cyclodextrin (TMCD) and its three clathrate compounds containing benzoic acid (BA), *p*-nitrobenzoic acid (NBA) and *p*-hydroxybenzoic acid (HBA), sucrose (SUC), salicin (SAL), phenolphthalein (PP), 1,3,5-tri-α-naphthylbenzene (TNB), *p*-quaterphenyl (*p*-QP), *p*-terphenyl (*p*-TP) and 1,3,5-triphenylbenzene (TPB). The amorphization was checked by X-ray powder diffraction and differential scanning calorimetry (DSC).[6-8] To investigate the thermal properties of the ground amorphous solids, the heat capacities of crystal, liquid-quenched glass (LQG), and ground amorphous solid (GAS) of TMCD[9] and TNB[10] were measured in the temperature range between 12 and 375 K. The significant results in these studies are surveyed in this paper. The grinding-time and grinding-temperature dependences on the enthalpy relaxation of TMCD are first reported in this paper.

EXPERIMENTAL

The commercial reagent of TMCD was purchased from TOSHIN CHEMICAL CO., LTD, those of BA, NBA, HBA, SUC, SAL, PP from TOKYO KASEI KOGYO CO., LTD, and those of *p*-QP, *p*-TP, TPB from Aldrich Chemical Co., Inc. TNB was offered by Dr. Nakano and Professor Shirota, Faculty of Engineering, Osaka University. These samples were all used without any further purification. The purities of the samples were checked to be better than 99 %.

The powder sample of about 5-8 cm^3 was ground for 2-16 h by using a vibrating mill TI100 (Heiko Manufacturing, LTD.) in dry nitrogen atmosphere at room temperature. This machine used a single cylindrical rod, in place of many balls usually employed, to pestle the sample, making it easy to take out the powdered sample of sticky nature from the pot. The pot and rod were made of aluminum oxide and the free space of the pot was about 10 cm^3. The surface temperature of the pot was kept below 40 °C during the milling. For TMCD, another milling experiment in which the pot temperature was kept below 25 °C was carried out to investigate the effect of the milling temperature.

LQG were prepared for TMCD, TMCD-BA, TMCD-NBA, TMCD-HBA, SUC, SAL, PP and TNB by cooling their melts from above the fusion temperature (T_{fus}) to room temperature. The estimated cooling rate was about 300 °C min^{-1}. *p*-QP, *p*-TP and TPB did not vitrify in a similar experiment.

The differential scanning calorimetry (DSC) was carried out in the heating direction using a Perkin-Elmer DSC 7. The samples were sealed in aluminum pans. The temperature range covered was between 30 °C and the temperature 10-20 °C higher than T_{fus}. The mass of the sample used was 3-7 mg and the heating rate was 3 °C min^{-1}.

The X-ray powder diffraction were taken at room temperature using a diffractometer model RAD-ROC (Rigaku Denki Co., Ltd.) at X-ray Diffraction Service of the Department of Chemistry, Faculty of Science, Osaka University. The sample of 0.2 mm thickness was mounted on the glass sample holder. The range of the diffraction angle 2θ was 3-60 deg and the scanning speed was 3 deg min^{-1}.

The heat capacities of LQG, GAS and crystal of TMCD and TNB were measured with adiabatic calorimeters described elsewhere.[11,12] The imprecision of the heat capacity was within 0.3 % in the temperature region $T < 15$ K, 0.1 % in 15 K $< T <$ 30 K, and 0.05 % in $T > 30$ K. The amount of the sample loaded in the cell was about 2 g for all of the compounds. Helium gas (760 torr at room temperature) was charged into the dead space of the cell (*ca.* 3 cm^3) to obtain good thermal contact between the cell and the sample.

RESULTS AND DISCUSSION

Solid State Amorphization by Vibrating Mill

The crystals of TMCD, TMCD-BA, TMCD-NBA, TMCD-HBA, SUC, SAL, PP and TNB were amorphized (partly in SUC, SAL and TNB) and those of *p*-QP, *p*-TP and TPB were not amorphized by the grinding for 2-4 h. TNB was amorphized completely on further grinding (16 h). For all of the amorphized samples, a halo pattern was observed in the X-ray powder diffraction. They were also characterized in the DSC thermogram by an exothermic peak due to the crystallization and an endothermic one due to the subsequent fusion. A step-like anomaly due to the glass transition was also observed in the DSC curves of TMCD, TMCD-BA, TMCD-NBA, TMCD-HBA and SUC. For other substances (SAL, PP and TNB), the crystallization occurred at the onset of the glass transition without fully delineating the C_p anomaly associated with the glass transition. The factor that determines the GAS forming ability is still unknown but it is pointed out that the GAS forming ability is strongly correlated with the glass forming ability by the ordinary liquid-quenching method.

For TMCD, which can be amorphized most easily among the molecular crystals studied, we investigated the grinding-time dependence of the X-ray diffraction pattern. Figure 1 shows the X-ray diffraction patterns for (a) the crystal before the grinding, (b) the sample ground for 5 min, and (c) the sample ground for 25 min. Bragg peaks in (a) and halo in (c) are evident. The overlapping Bragg peaks and halos were observed in Figure 1(b). The positions and relative intensities of the Bragg peaks are essentially the same as those shown in Figure 1(a), indicating coexistence of the crystalline and amorphous solids. The intensity of the Bragg peaks decreased as the sample was ground

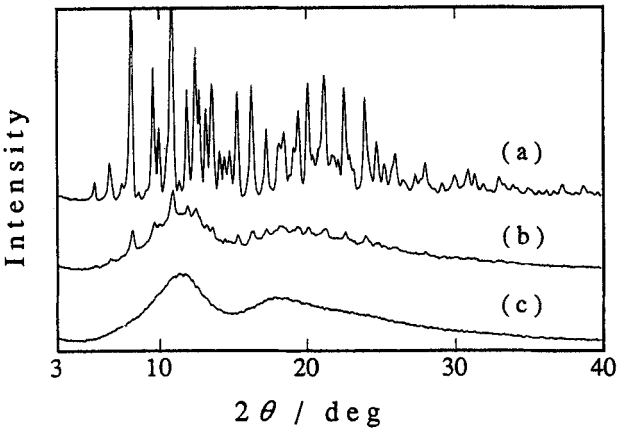

FIGURE 1 X-ray powder diffraction patterns of TMCD: (a) crystal, (b) GAS (5 min), (c) GAS (25 min).

further and disappeared completely for the 25 min sample (Figure 1(c)). After 25 min, the diffraction pattern did not change on further grinding. Figure 2 shows the X-ray

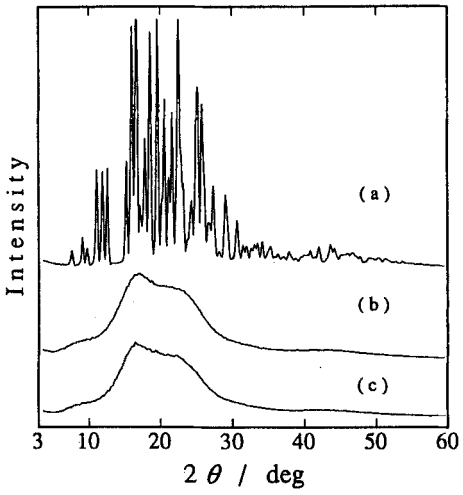

FIGURE 2 X-ray powder diffraction patterns of TNB: (a) crystal, (b) LQG, (c) GAS.

diffraction patterns of TNB; (a) crystal, (b) LQG, (c) GAS for 16 h. The Bragg peaks observed in the crystal (Figure 2(a)) completely disappeared and replaced a halo pattern in GAS (Figure 2(c)). There was no distinct difference between the diffraction patterns of LQG (b) and GAS (c).

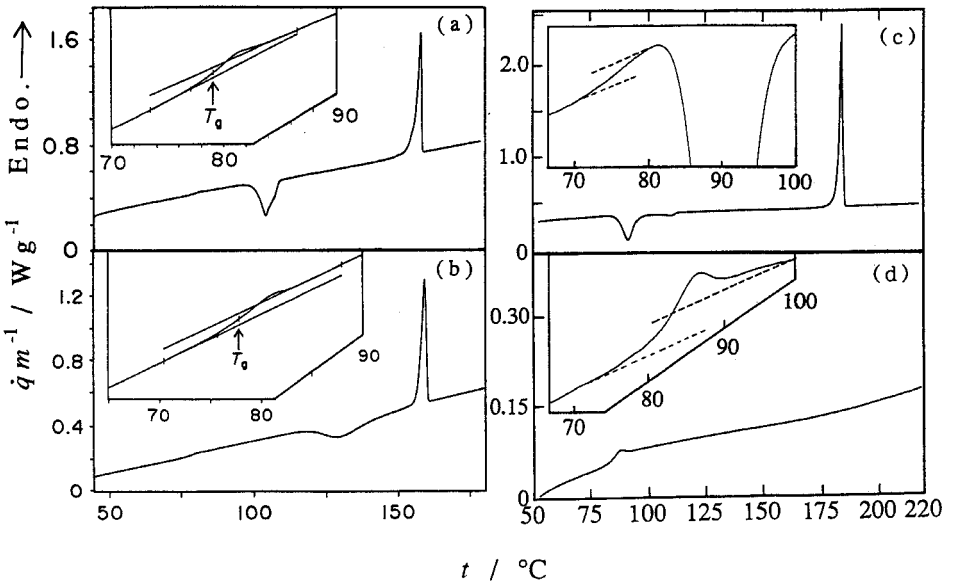

FIGURE 3 DSC curves of TMCD ((a) GAS, (b) LQG) and TNB ((c) GAS, (d) LQG).

Figure 3 shows the DSC curves of TMCD ((a) and (b)) and TNB ((c) and (d)). The upper figures ((a) and ((c)) are for GAS and the lower ones for LQG. In GAS of TMCD, a step-like anomaly due to the glass transition appeared at the same temperature as T_g of LQG (78 °C) and an exothermic peak due to the crystallization around 110 °C. In GAS of TNB, however, the crystallization occurred at the onset of the glass transition as shown in the inset of (c). The onset temperature of the glass transition in GAS was close to that of LQG (72 °C). It is interesting that the ease with which crystallization occurs in the LQG samples was opposite to that in the GAS samples; no crystallization occurred in LQG of TNB. Both the remaining nuclei and the structure of GAS may be involved with the complicated crystallization phenomena. The samples crystallized from GAS melted at the same temperatures as the original crystals, indicating that both samples remained chemically stable all through the vigorous grinding.

Heat Capacities and Glass Transitions of the Amorphized Solids

The molar heat capacities of TMCD are shown in Figure 4. The closed circles, open circles and triangles correspond to the data for GAS (for 4 h), LQG and crystalline samples, respectively. A large heat capacity jump of 0.3 kJ K^{-1}mol^{-1} appeared at 345 K for both GAS and LQG samples. These are due to the glass transitions observed in the DSC experiments. The calorimetric glass transition temperature (345 K) was slightly

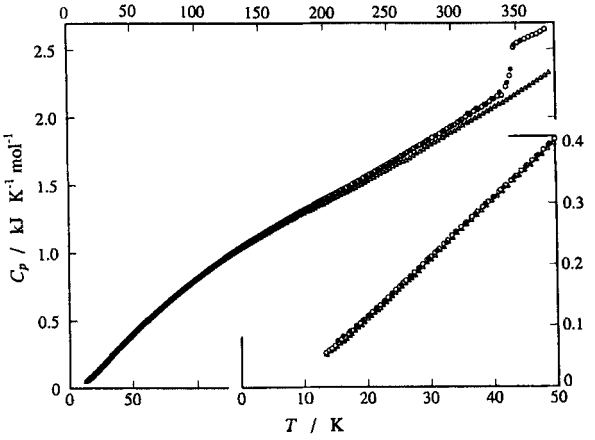

FIGURE 4 Heat capacities of TMCD. Open circles: LQG, closed circles: GAS, triangles: crystal.

smaller than T_g determined by DSC (351 K) and is explained as usual by the difference in the effective heating rate of the two experiments. The heat capacity of GAS was close to that of LQG in the whole temperature range including the glass transition region. Heat capacity of the crystal was measured with the sample obtained by annealing GAS at 360 K for 1 day. The heat capacity of the crystal were 2-3 % smaller than those of LQG as frequently observed in the glass-forming materials.

Figure 5 shows the molar heat capacities of TNB. The symbols (closed circle, open

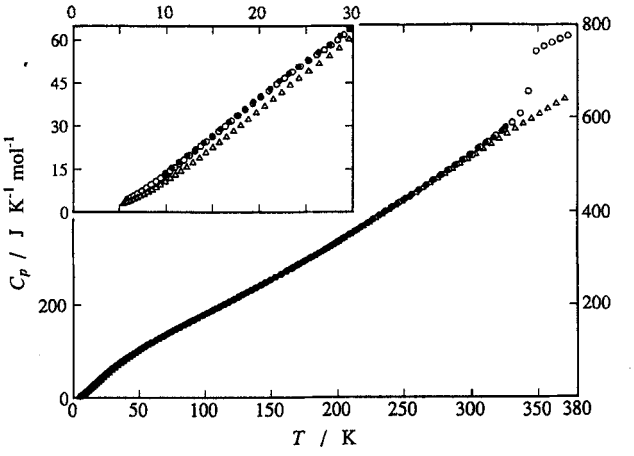

FIGURE 5 Heat capacities of TNB. Open circles: LQG, closed circles: GAS, triangles: crystal.

circle, triangle) represent the data for GAS (for 16 h), LQG and crystalline samples, respectively. In LQG, a large heat capacity jump (ΔC_p = 150 J $K^{-1}mol^{-1}$) appeared at around 340 K, which is smaller than T_g determined by DSC (355 K). The crystallization of the LQG did not occur up to the highest temperature of this experiment (375 K). The heat capacity of GAS was almost the same as that of LQG as in the case of TMCD. The glass transition of GAS could not be observed because the crystallization began at around 320 K, which is about 25 K lower than T_g of LQG (342 K). The heat capacity of the crystal was measured using the sample obtained by annealing the GAS at around 360 K for 17 h. The heat capacity of the crystal were 0.5-1 % smaller than those of LQG.

Enthalpy Relaxation and its Grinding-time and Grinding-temperature Dependence

Figure 6 shows the enthalpy relaxation rate dH_c/dt observed during each equilibration

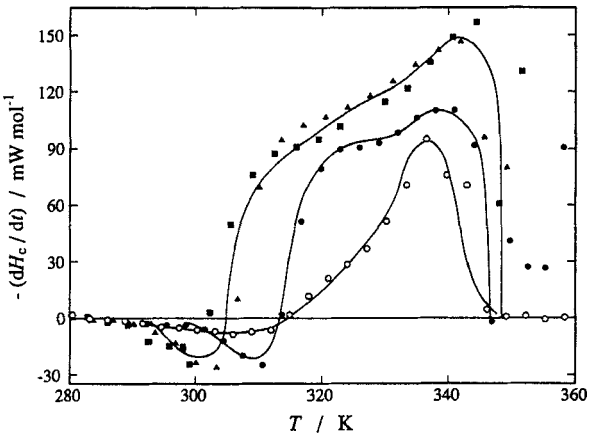

FIGURE 6 Relaxation rates of configurational enthalpy of TMCD. Open circles: LQG, closed circles: GAS (40 °C, 4 h), closed triangles: GAS (25 °C, 4 h), closed squares: GAS (25 °C, 1 h).

period in the heat capacity measurement of TMCD. This quantity was evaluated by multiplying the spontaneous temperature drift rate by the heat capacity of the sample including the sample cell. The drift rate was measured at 10 min after each energy input. This time (10 min) was sufficiently long for thermal equilibration in the normal region. The symbols (open circle, closed circle, closed triangle, closed square) correspond to LQG, GAS (40 °C, 4 h), GAS (25 °C, 4 h), and GAS (25 °C, 1 h), respectively. In LQG, a slight endothermic temperature drift followed by large exothermic one was observed below T_g. The temperature dependence and temperature width of this exothermic effect are similar to those of the standard glass transitions of molecular

liquids.[13,14] However, the temperature dependence of the exothermic effect of GAS (closed symbols) was quite unusual; larger and almost constant exothermic temperature drifts were observed in the wide temperature range. It is noted that the sample ground at 25 °C exhibited larger exothermic drift than that at 40 °C and its starting temperature was about 15 K lower than that of the sample at 40 °C. The difference between the samples ground at 25 °C for 4 h and 1 h was quite small. The irregular data points of GAS just above T_g (closed symbols in Figure 6) correspond to the crystallization process.

In the temperature region where the exothermic effect occurred in the heat capacity measurement, the sample was relaxing towards the equilibrium undercooled liquid by releasing an excess enthalpy. This enthalpy, which is referred to as configurational enthalpy, is associated with the configurational change of the TMCD molecules. The temperature and time dependence of the configurational enthalpy $H_c(T,t)$ is evaluated by

$$H_c(T,t) = \sum (dH_c/dt)\,\Delta t,$$

where (dH_c/dt) is the enthalpy relaxation rate plotted in Figure 6 and Δt the time between the midpoints of two successive energy input periods (about 40 min).

Figure 7 shows the temperature dependence of the configurational enthalpy

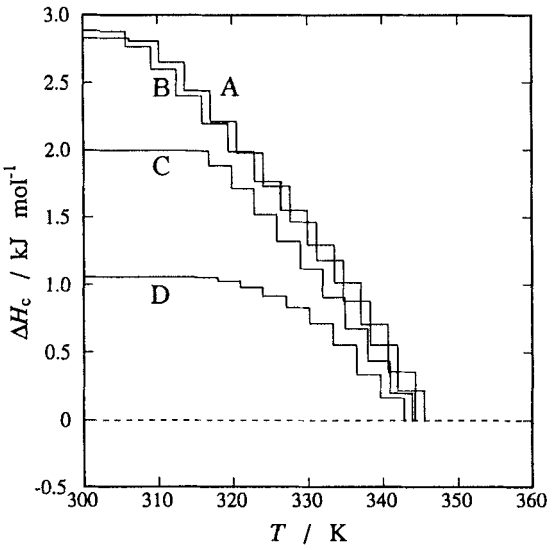

FIGURE 7 Relaxation processes of configurational enthalpy of TMCD. A: GAS (25 °C, 4 h), B: GAS (25 °C, 1 h), C: GAS (40 °C, 4 h), D: LQG.

calculated by this method. The four step-like lines A, B, C, and D correspond to GAS (25 °C, 4 h), GAS (25 °C, 1 h), GAS (40 °C, 4 h), and LQG, respectively. The horizontal segments represent the temperature increase due to the electrical heating which

is assumed to have taken infinitesimally short periods. The vertical ones represent the amount of enthalpy relaxed. The origin of $H_c(T,t)$ was taken at the temperature at which each sample reached the equilibrium state during the heat capacity measurement. It was found that GAS (40 °C, 4 h) had about twice larger ΔH_c than LQG and GAS (25 °C, 4 h) and GAS (25 °C, 1 h) had about three times larger ΔH_c than LQG at the initial stage of the relaxation. The relaxation rate on heating depended on the ΔH_c value; it was larger for the larger initial value of ΔH_c. The three curves representing the different GAS samples all approached to that of LQG just below T_g (345 K), indicating that all of the samples were in a similar states at T_g. This may be the reason why T_g of GAS was the same as that of LQG in the calorimetric experiments (DSC and adiabatic calorimetry).

Supposing that we can define entropy for GAS as well as for LQG, larger configurational enthalpy may naturally be associated with larger configurational entropy. We may therefore conclude that GAS is more strained (large enthalpy) and disordered (large entropy) state than LQG from the thermodynamic point of view. It is also pointed out that the strained and disordered state of GAS depends on the grinding temperature more sensitively than on the grinding time. This observation can be explained qualitatively by the Adam-Gibbs theory.[15] This theory asserts that the relaxation time τ of the structural change in liquids is controlled by the configurational entropy S_c as well as by the temperature T according to the following equation,

$$\tau = A \exp(B/TS_c),$$

where A and B are constants. If the sample is ground vigorously and long enough, any large-enthalpy and large-entropy states will relax to the state with the relaxation time of our experimental time scale (10-100 ks) during grinding and in the period before the heat capacity measurement. The relaxation time is determined by the product TS_c so that larger entropy (enthalpy) states are generated by grinding at lower temperatures and the same entropy state is generated at the same grinding temperature independently of the grinding time. The Adam-Gibbs equation also explains the experimental result that larger enthalpy states (GAS) relaxed faster than smaller enthalpy states (LQG).

Among the further studies of GAS will be investigations of the disordered and strained structure of GAS using X-ray and neutron diffraction. TNB should be a good candidate for such structural studies because of its intrinsic simplicity of the molecular shape.

ACKNOWLEDGMENT

The authors thank Professor Yasuhiko Shirota and Dr. Hideyuki Nakano, Faculty of Engineering, Osaka University for their effort to prepare TNB crystal of high quality. The

authors also thank the research group of Professor Yoshinobu Nakai, Faculty of Pharmaceutical Science, Chiba University, for their kind advice for the grinding-amorphization method. The authors are deeply indebted to Mr. Tetsuo Yamamoto for his help in the X-ray diffraction experiment. This work was supported by a Grant-in-Aid for Scientific Research No. 06804032 from the Ministry of Education, Science and Culture.

REFERENCES

* Contribution No. 116 from the Microcalorimetry Research Center.
1. Solid State Amorphizing Transformations (J. Less-Common Met., 140), edited by R. B. Schwarz and W. L. Johnson (1988).
2. Structure of Non-crystalline Materials (J. Non-Cryst. Solids, 150), edited by K. Suzuki and A. C. Wright (1992), Sect. 12.
3. For example: Z. Hen, J. Phys.: Condens. Matter, 5, L337 (1993); M. J. Bernal, M. M. dela Cruz, R. Pareja, and J. M. Riveiro, J. Non-Cryst. Solids, 180, 164 (1995).
4. For example: A. C. Wright, B. Bachra, T. M. Brunier, R. N. Sinclair, L. F. Gladden, and R. L. Portsmouth, J. Non-Cryst. Solids, 150, 69 (1992); J. P. Bonnet, M. Boissier, and A. A. Gherbi, J. Non-Cryst. Solids, 167, 199 (1994).
5. Y. Nakai, K. Yamamoto, and K. Terada, J. Incl. Phenom., 2, 523 (1984).
6. I. Tsukushi, O. Yamamuro, and H. Suga, J. Therm. Anal., 37, 1359 (1991).
7. I. Tsukushi, O. Yamamuro, and H. Suga, Thermochim. Acta, 200, 71 (1992).
8. I. Tsukushi, O. Yamamuro, and T. Matsuo, Solid State Commun., 94, 1013 (1995).
9. I. Tsukushi, O. Yamamuro, and H. Suga, J. Non-Cryst. Solids, 175, 187 (1994).
10. I. Tsukushi, O. Yamamuro, T. Ohta, T. Matsuo, H. Nakano, and Y. Shirota, J. Phys.: Condens. Matter, submitted.
11. K. Moriya, T. Matsuo, and H. Suga, J. Chem. Thermodyn., 14, 1143 (1982).
12. O. Yamamuro, M. Oguni, T. Matsuo, and H. Suga, Bull. Chem. Soc. Jpn., 60, 1269 (1987).
13. H. Suga and S. Seki, J. Non-Cryst. Solids, 16, 171 (1974).
14. H. Suga, J. Chim. Phys. Phys.-Chim. Biol., 82, 275 (1985).
15. G. Adam and J. H. Gibbs, J. Chem. Phys., 43, 139 (1965).